Journal of Sound and Vibration 571 (2024) 118068

Contents lists available at ScienceDirect

Journal of Sound and Vibration

journal homepage: www.elsevier.com/locate/jsvi

A novel demodulation method with a reference signal for operational modal analysis and baseline-free damage detection of a beam under random excitation

L.F. Lyu, K. Yuan, W.D. Zhu *

Department of Mechanical Engineering, University of Maryland, Baltimore County, 1000 Hilltop Circle, Baltimore, MD 21250, USA

ARTICLE INFO

Keywords:
Continuously scanning laser Doppler vibrometer system
Demodulation method
Random excitation
Cross-correlation function
Baseline-free damage detection

ABSTRACT

A novel demodulation method with a reference signal is developed for operational modal analysis and damage detection of a beam structure under random excitation. The novel demodulation method can process measurements of the beam by a continuously scanning laser Doppler vibrometer (CSLDV) system and measurements of a reference point on the beam by a single-point laser Doppler vibrometer to estimate its modal parameters, such as damped natural frequencies and undamped mode shapes. Damped natural frequencies of the beam are estimated from fast Fourier transforms of measurements of the CSLDV system. A cross-correlation function between a measurement of the CSLDV system and a measurement of a single-point laser Doppler vibrometer is calculated, and the cross-correlation function is multiplied by a sinusoidal signal whose frequency is an estimated damped natural frequency of the beam. The processed cross-correlation function is filtered by a low-pass filter to obtain the undamped mode shape of the beam that corresponds to the estimated damped natural frequency of the beam. Smooth polynomials are used to fit estimated undamped mode shapes, which can be considered as undamped mode shapes of an undamaged beam. Curvatures of estimated undamped mode shapes and polynomials are compared by curvature damage indices to determine the location of a damage in the beam. The novel demodulation method with a reference signal is investigated for baseline-free damage detection from both finite element simulation and experiment. Modal parameters of a finite element model of the damaged beam and a damaged beam specimen, which are under random excitation, are successfully estimated, and locations of damages in the beam model and beam specimen are accurately determined.

Introduction

The dynamic behavior of a structure can be affected by a damage in it, and one can detect the occurrence of a damage by studying the dynamic behavior of the structure.[1] Modal parameters, such as damped natural frequencies and undamped mode shapes, of the structure are used to describe its dynamic behavior, which are useful for damage detection. Modal parameters of a structure can be estimated by modal analysis, which includes experimental modal analysis (EMA) and operational modal analysis (OMA).[2] EMA requires excitation measurement while OMA does not; thus OMA is more appropriate for a structure under an operational condition or

* Corresponding author.
E-mail address: wzhu@umbc.edu (W.D. Zhu).

https://doi.org/10.1016/j.jsv.2023.118068
Received 15 May 2023; Received in revised form 12 July 2023; Accepted 28 September 2023
Available online 2 October 2023

under random excitation. Different damage detection methods were developed based on modal analysis.[3-5] Valdes and Soutis[3] studied the effect of delamination in a composite beam on its natural frequencies. Lestari et al.[4] used piezoelectric sensors to estimate curvature mode shapes of intact and damaged beams, and detected different types of damage in beams by comparing estimated curvature mode shapes of intact and damaged beams. He et al.[5] used curvature mode differences between intact and damaged beams to identify the number and degrees of damages. However, baseline information from undamaged test samples were needed in the above methods, and contact-type sensors were used in their tests, which can introduce mass loadings to test structures and affect their estimated modal parameters.

A laser Doppler vibrometer, which can accurately measure the surface velocity of a point on a structure, provides an efficient and non-contact way for OMA of the structure.[6] However, it is difficult to use the laser Doppler vibrometer to measure vibrations of multiple points on the structure, and a scanning laser Doppler vibrometer (SLDV) system was developed to provide measurements with a high spatial resolution.[6-8] A scanner with a set of orthogonal mirrors was integrated into the SLDV system, and rotation angles of the mirrors could be controlled so that the laser spot of the SLDV system was moved to a desired position on the structure. The SLDV system measures the vibration of a point for a period of time and then moves its laser spot to the next point.[9,10] To increase the efficiency for measuring a large number of points on the structure, a continuously scanning laser Doppler vibrometer (CSLDV) system was developed.[11-14] Mirrors of a scanner in the CSLDV system continuously rotate so that the laser spot of the CSLDV system is swept along a prescribed trajectory on a structure. Recently, novel CSLDV systems including a tracking CSLDV[15,16] and a three-dimensional (3D) CSLDV[17-21] were developed to accurately estimate transverse mode shapes of a rotating fan blade and 3D mode shapes, which include in-plane mode shapes,[19] of stationary structures with flat[17-19] and curved[20,21] surfaces, respectively, which significantly extended application areas of CSLDV systems.

Different OMA methods have been developed to process responses from CSLDV measurements of structures to estimate their modal parameters, including natural frequencies, damping ratios, and mode shapes, and operational deflection shapes (ODSs).[22-27] A demodulation method and a polynomial method were developed to estimate ODSs of a structure subject to sinusoidal excitation.[22,23] Estimated ODSs and their curvatures (CODSs) of a beam under sinusoidal excitation can be used for identifying a damage in it via a novel damage detection method with a curvature damage index (CDI).[28] The method is baseline-free since a polynomial with a proper order to fit ODSs of the structure from the demodulation method is used to simulate an associated undamaged structure. By designing a two-dimensional (2D) scan scheme on a plate with a thickness reduction damage, its full-field ODSs under sinusoidal excitation were estimated via CSLDV measurements, and the location of the damage was determined via the baseline-free damage detection method that was extended from one dimension to two dimensions.[29] The method was also used to accurately locate delaminations in composite plates.[30,31] A damage detection method using modal rotational ODSs of a plate obtained from its CSLDV measurements was developed to locate cracks near its edge.[32] However, the above methods are not suitable for structures under random excitation, which is the most practical excitation in real-world applications, since the demodulation method can only be used to process responses from CSLDV measurements of structures under sinusoidal excitation.

A lifting method was developed to estimate undamped modes shapes of a structure under random excitation.[27] Estimated undamped mode shapes from the lifting method can be used for baseline-free damage detection. However, the Nyquist frequency of the CSLDV system when using the lifting method depends on the scan frequency, which is the number of times the CSLDV system completes a back-and-forth scan in one second. It is difficult to use the lifting method for OMA of a structure with high natural frequencies. Recently, a new OMA method for CSLDV measurements was developed to improve the traditional demodulation method to estimate undamped mode shapes of structures under random excitation, where a high scan frequency of the CSLDV system was not needed.[18,33,34] However, estimated undamped mode shapes of structures using the improved demodulation method are not suitable for their baseline-free damage detection since bandpass filters are used to pre-process and smooth their measured responses.

In this work, a new OMA method based on a novel demodulation method with a reference signal is developed for estimating undamped mode shapes of a structure under random excitation. The novel demodulation method processes correlation functions between measurements of the CSLDV system and measurements of a reference sensor. Estimated 1D undamped mode shapes can be processed by the baseline-free damage detection method to identify locations of damages in the structure. Both finite element method (FEM) simulations and experimental tests are conducted to validate the new OMA method and baseline-free damage detection method, and locations of damages in structures are successfully identified.

Remaining sections of this work are listed below. A correlation function between a CSLDV measurement and a measured reference signal is introduced in Section 'Correlation function between a CSLDV measurement and a measured reference signal', a demodulation method for the correlation function is introduced in Section 'Demodulation method for the correlation function', and a baseline-free damage detection method is introduced in Section 'Baseline-free damage detection method'. A finite element model of a damaged beam is introduced in Section 'Finite element model', and simulation results of the finite element model are presented in Section 'Finite element simulation results'. An experimental setup is introduced in Section 'Experimental setup', modal parameter estimation and damage detection results are presented in Section 'Experimental results of modal parameter estimation and damage detection'. Some conclusions are presented in Section 'Conclusion'.

Methodology

Correlation function between a CSLDV measurement and a measured reference signal

When white-noise excitation is applied at point q of a linear time-invariant structure, its response at time t can be expressed by (Xu et al.[27])

$$u(t) = \sum_{i=1}^{N} \phi_i \int_{-\infty}^{t} \phi_{i,q} f_q(t) g_i(t-\tau) \mathrm{d}\tau \tag{1}$$

where $\phi_{i,q}$ and f_q denote the entry of the i th undamped mode shape of the structure ϕ_i corresponding to q and white-noise excitation at q, respectively, and $g_i(t) = \frac{1}{\omega_{i,d}} \mathrm{e}^{-\zeta_i \omega_i t} \sin(\omega_{i,d} t)$ in which $\omega_{i,d}$ is the i th damped natural frequency, ζ_i is the i th modal damping ratio, and ω_i is the i th undamped natural frequency. The response of the structure at point p can be expressed by

$$u_p(t) = \sum_{i=1}^{N} \phi_{i,p} \int_{-\infty}^{t} \phi_{i,q} f_q(t) g_i(t-\tau) \mathrm{d}\tau \tag{2}$$

where $\phi_{i,p}$ denotes the entry of ϕ_i corresponding to p. When a CSLDV system measures the response of the structure along an arbitrary scan path $\mathbf{s}$ assigned on a surface of the structure, the laser spot of the system sweeps along $\mathbf{s}$, and the measured response can be expressed by

$$u_s(t) = \sum_{i=1}^{N} \widetilde{\phi}_{i,\mathbf{s}(t)} \int_{-\infty}^{t} \phi_{i,q} f_q(t) g_i(t-\tau) \mathrm{d}\tau \tag{3}$$

where $\widetilde{\phi}_{i,\mathbf{s}}$ is a function of t and denotes the entry of ϕ_i corresponding to a point on the structure, at which the laser spot arrives at time t.

A cross-correlation function between $u_p(t)$ and $u_\mathbf{s}(t)$ can be calculated as the expected value of their product. The cross-correlation function with $u_p(t)$ and $u_\mathbf{s}(t)$ serving as reference and measurement data, respectively, can be expressed by

$$R_{psq}\left[u_p(t_1), u_\mathbf{s}(t_2)\right] = E\left[u_p(t_1) u_\mathbf{s}(t_2)\right] \tag{4}$$

where E[·] is the expectation operator, and t_1 and t_2 are two time variables corresponding to $u_p(t)$ and $u_\mathbf{s}(t)$, respectively. Let T be a time-delay variable; one has $t_2 = t_1 + T$, and Eq. (4) becomes

$$R_{psq}(t_1, T) = E\left[u_p(t_1) u_\mathbf{s}(t_1 + T)\right] \tag{5}$$

Substituting Eqs. (2) and (3) into Eq. (5) yields

$$R_{psq}(t_1, T) = E\left[\sum_{i=1}^{N} \sum_{j=1}^{N} \phi_{i,q} \phi_{i,p} \phi_{j,q} \widetilde{\phi}_{j,s(t_1+T)} \int_{-\infty}^{t_1} \int_{-\infty}^{t_1+T} g_i(t_1-\sigma) g_j(t_1+T-\tau) f_q(\sigma) f_q(\tau) \mathrm{d}\sigma \mathrm{d}\tau\right] \tag{6}$$

Since only f is random in Eq. (6), it can be rewritten as

$$R_{psq}(t_1, T) = \sum_{i=1}^{N} \sum_{j=1}^{N} \phi_{i,q} \phi_{i,p} \phi_{j,q} \widetilde{\phi}_{j,\mathbf{s}(t_1+T)} \int_{-\infty}^{t_1} \int_{-\infty}^{t_1+T} g_i(t_1-\sigma) g_j(t_1+T-\tau) \mathrm{E}\left[f_q(\sigma) f_q(\tau)\right] \mathrm{d}\sigma \mathrm{d}\tau \tag{7}$$

The expected value of $f_q(\sigma) f_q(\tau)$ can be expressed by

$$\mathrm{E}\left[f_q(\sigma) f_q(\tau)\right] = \alpha_q \delta(\tau - \sigma) \tag{8}$$

where α_q is a constant associated with f_q and δ is the Dirac delta function. Substituting Eq. (8) into Eq. (7) yields

$$R_{psq}(t_1, T) = \sum_{i=1}^{N} \sum_{j=1}^{N} \alpha_q \phi_{i,q} \phi_{i,p} \phi_{j,q} \widetilde{\phi}_{j,\mathbf{s}(t_1+T)} \int_{-\infty}^{t_1} g_i(t_1-\sigma) g_j(t_1+T-\sigma) \mathrm{d}\sigma \tag{9}$$

Let $\lambda = t_1 - \sigma$; one has

$$R_{psq}(t_1, T) = \sum_{i=1}^{N} \sum_{j=1}^{N} \alpha_q \phi_{i,q} \phi_{i,p} \phi_{j,q} \widetilde{\phi}_{j,\mathbf{s}(t_1+T)} \int_{0}^{+\infty} g_i(\lambda) g_j(T+\lambda) \mathrm{d}\lambda \tag{10}$$

Substituting $g_i(t) = \frac{1}{\omega_{i,d}} \mathrm{e}^{-\zeta_i \omega_i t} \sin(\omega_{i,d} t)$ into Eq. (10) yields

$$R_{psq}(t_1, T) = \sum_{j=1}^{N} A_j \widetilde{\phi}_{j,\mathbf{s}(t_1+T)} \mathrm{e}^{-\zeta_i \omega_i T} \cos\left(\omega_{j,d} T - \theta_j\right) \tag{11}$$

where A_j is an amplitude constant, and θ_j is a phase constant.

The cross-correlation function R_{psq} in Eq. (11) is different from that between responses of two fixed points, e.g., p and r, of the structure in that the former has two independent time variables, i.e., t_1 and T, and the latter has only one time-delay variable, i.e., T. The reason is that both u_p and u_r are wide-sense stationary, as both $\mathrm{E}[u_p]$ and $\mathrm{E}[u_q]$ are constants and independent of t. However, $u_{\mathbf{s}}(t)$ is not wide-sense stationary, as $\mathrm{E}[u_q]$ is not a constant and depends on t due to continuous scanning of the CSLDV system.

This completes the theoretical derivation of a cross-correlation function between the response measured by a CSLDV system and that of a fixed point of a linear, time-invariant structure under white-noise excitation applied at a fixed point. Since the structure is linear, the superposition principle can be applied. The response of the structure under white-noise excitation applied at multiple points on it can be expressed as a sum of multiple responses under white-noise excitation applied at all the points. The resulting summed cross-correlation function has the same expression as that in Eq. (11), with the same mode shape $\widetilde{\phi}$ and different A_j and θ_j.

Demodulation method for the correlation function

The correlation function R_{psq} can be written as

$$R_{psq}(t_1,T)=\sum_{j=1}^{N}C_j(T)\widetilde{\phi}^{i}_{j,\mathbf{s}(t_1+T)}\cos(\omega_{j,d}T)+D_j(T)\widetilde{\phi}^{q}_{j,\mathbf{s}(t_1+T)}\sin(\omega_{j,d}T) \tag{12}$$

where $C_j(T)$ and $D_j(T)$ are two coefficients, and $\widetilde{\phi}^{i}_{j,\mathbf{s}(t_1+T)}$ and $\widetilde{\phi}^{q}_{j,\mathbf{s}(t_1+T)}$ are in-phase and quadrature components of $\widetilde{\phi}_{j,\mathbf{s}(t_1+T)}$, respectively. The correlation function is multiplied by a sinusoidal signal $\cos(\omega_{k,d}T)$ where $\omega_{k,d}$ is the k-th damped natural frequency of the structure:

$$\begin{aligned}
&\sum_{j=1}^{N}C_j(T)\widetilde{\phi}^{i}_{j,\mathbf{s}(t_1+T)}\cos(\omega_{j,d}T)\cos(\omega_{k,d}T)+D_j(T)\widetilde{\phi}^{q}_{j,\mathbf{s}(t_1+T)}\sin(\omega_{j,d}T)\cos(\omega_{k,d}T)\\
&=C_k(T)\widetilde{\phi}^{i}_{j,\mathbf{s}(t_1+T)}\cos^2(\omega_{k,d}T)+D_k(T)\widetilde{\phi}^{q}_{j,\mathbf{s}(t_1+T)}\sin(\omega_{k,d}T)\cos(\omega_{k,d}T)\\
&+\sum_{j=1}^{k-1}C_j(T)\widetilde{\phi}^{i}_{j,\mathbf{s}(t_1+T)}\cos(\omega_{j,d}T)\cos(\omega_{k,d}T)+D_j(T)\widetilde{\phi}^{q}_{j,\mathbf{s}(t_1+T)}\sin(\omega_{j,d}T)\cos(\omega_{k,d}T)\\
&+\sum_{j=k+1}^{N}C_j(T)\widetilde{\phi}^{i}_{j,\mathbf{s}(t_1+T)}\cos(\omega_{j,d}T)\cos(\omega_{k,d}T)+D_j(T)\widetilde{\phi}^{q}_{j,\mathbf{s}(t_1+T)}\sin(\omega_{j,d}T)\cos(\omega_{k,d}T)
\end{aligned} \tag{13}$$

The k-th damped natural frequency of the structure can be determined by applying the fast Fourier transform to R_{psq}. By using the double-angle formula, one has

$$C_k(T)\widetilde{\phi}^{i}_{j,\mathbf{s}(t_1+T)}\cos^2(\omega_{k,d}T)=\frac{1}{2}C_k(T)\widetilde{\phi}^{i}_{j,\mathbf{s}(t_1+T)}+\frac{1}{2}C_k(T)\widetilde{\phi}^{i}_{j,\mathbf{s}(t_1+T)}\cos(2\omega_{k,d}T) \tag{14}$$

By applying a low-pass filter to Eq. (13), the term $\widetilde{\phi}^{i}_{j,\mathbf{s}(t_1+T)}$ can be extracted based on Eq. (14). Similarly, one can multiply Eq. (12) by a sinusoidal signal $\sin(\omega_{k,d}T)$ to extract $\widetilde{\phi}^{q}_{j,\mathbf{s}(t_1+T)}$. Once $\widetilde{\phi}^{i}_{j,\mathbf{s}(t_1+T)}$ and $\widetilde{\phi}^{q}_{j,\mathbf{s}(t_1+T)}$ are obtained, one can estimate $\widetilde{\phi}_{j,\mathbf{s}(t_1+T)}$, which is the undamped mode shape of the structure on the scan path $\mathbf{s}$.

Baseline-free damage detection method

The curvature of $\widetilde{\phi}_{j,\mathbf{s}(t_1+T)}$ can be calculated by

$$\widetilde{\phi}''_{j,\mathbf{s}(t_1+T)}=\frac{\mathrm{d}^2\widetilde{\phi}_{j,\mathbf{s}(t_1+T)}}{\mathrm{d}x^2} \tag{15}$$

where x denotes a spatial position along the scan path $\mathbf{s}$. The polynomial fit of $\widetilde{\phi}_{j,\mathbf{s}(t_1+T)}$ can be calculated as a baseline[27]:

$$\widetilde{\phi}^{p}_{j,\mathbf{s}(t_1+T)}=\sum_{h=0}^{r}\beta_h x^h \tag{16}$$

where h is a natural number, β_h is a constant coefficient corresponding to x^h, and r is the degree of the polynomial fit. The methods for determining a proper r and calculating β_h have been discussed in Ref. [27]. Differences between curvatures of $\widetilde{\phi}_{j,\mathbf{s}(t_1+T)}$ and the polynomial fit can be obtained by

$$\delta=\left[\widetilde{\phi}''_{j,\mathbf{s}(t_1+T)}-\left(\sum_{h=0}^{r}\beta_h h^2 x^{h-2}\right)\right]^2 \tag{17}$$

where δ is a CDI. Locations of damages in the structure can be identified in neighborhoods with high values in CDIs that correspond to

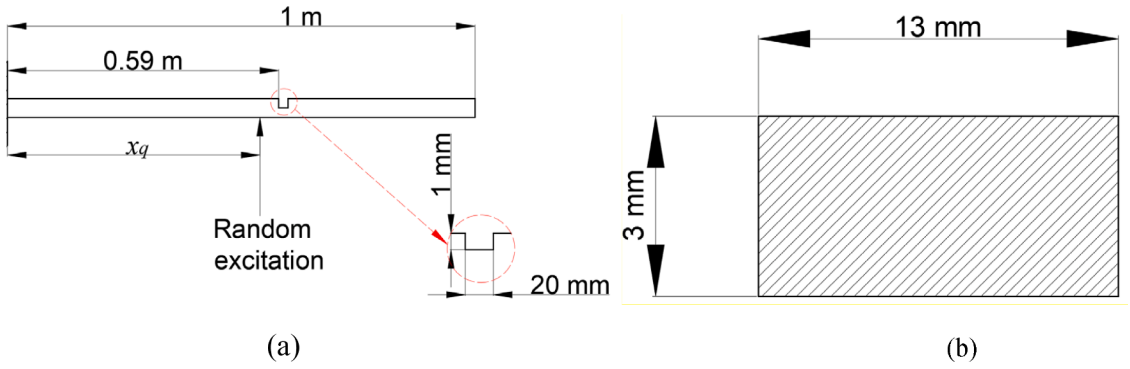

Fig. 1. (a) Schematic of the beam, and (b) the intact section of the beam.

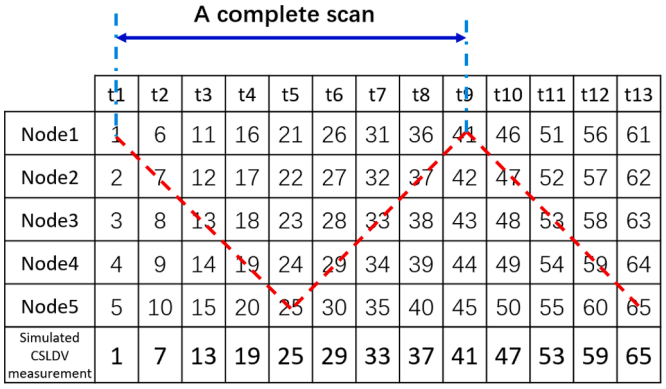

	t1	t2	t3	t4	t5	t6	t7	t8	t9	t10	t11	t12	t13
Node1	1	6	11	16	21	26	31	36	41	46	51	56	61
Node2	2	7	12	17	22	27	32	37	42	47	52	57	62
Node3	3	8	13	18	23	28	33	38	43	48	53	58	63
Node4	4	9	14	19	24	29	34	39	44	49	54	59	64
Node5	5	10	15	20	25	30	35	40	45	50	55	60	65
Simulated CSLDV measurement	1	7	13	19	25	29	33	37	41	47	53	59	65

Fig. 2. Preprocess of simulated responses from the finite element model.

different $\widetilde{\phi}_{j,s(t_1+T)}$. Note that signal-to-noise ratios of the measured response of a structure under random excitation can be low, and the neighborhoods with high values in estimated CDIs can be caused by noise. To remove noise in estimated CDIs and increase the accuracy of damage location identification, multiple estimated CDIs can be averaged by

$$\delta_a = \frac{1}{m}\sum_{l=1}^{m}\frac{\delta_l}{\delta_{l,max}} \tag{18}$$

where $l = 1,2,\ldots,m$, with m being the number of estimated CDIs, δ_a is an averaged and normalized CDI, δ_l is the l-th estimated CDI, and $\delta_{l,max}$ is the maximum value of δ_l.

Finite element simulation

Finite element model

To validate the demodulation method with a reference signal, a finite element model of a damaged cantilever beam was developed in ABAQUS. The model was an Aluminum Euler-Bernoulli cantilever beam with a rectangular section of 13 mm × 3 mm and a length of 1 m (Fig. 1). The Young's modulus of the beam was set to 70×10^9 Pa, the density of the beam was set to 2700 kg/m^3, and the Poisson's ratio of the beam was set to 0.35. There was a thickness reduction region with a depth of 1 mm and a length of 20 mm along the length of the beam (Fig. 1(a)). The distance between the clamped end of the beam and the left end of the thickness reduction region was 0.59 m (Fig. 1(a)).

Beam elements were used for modeling the beam, and 500 elements with the same size were assigned to the finite element model. A concentrated random force excitation with a maximum value of 0.2 N and a standard deviation of 0.0558 was applied to a node of an element of the finite element model. The distance between the node and the fixed end of the finite element model is x_q. Nodes of the finite element model are considered as measurement points of a CSLDV system. The distance between a measurement point on the scan line and its start point was x and the total length of the scan line was L. A non-dimensional parameter $\eta = x/L$, whose scale was from 0 to 1, was used to describe the location of a measurement point on the scan line. Simulated velocity responses of the beam were preprocessed to simulate measured responses of the CSLDV system when scanning back and forth along a straight line. A sample of preprocessing simulated responses is shown in Fig. 2. Simulated responses of 5 nodes at 13 instants form a matrix, where t1, t2, …, t13

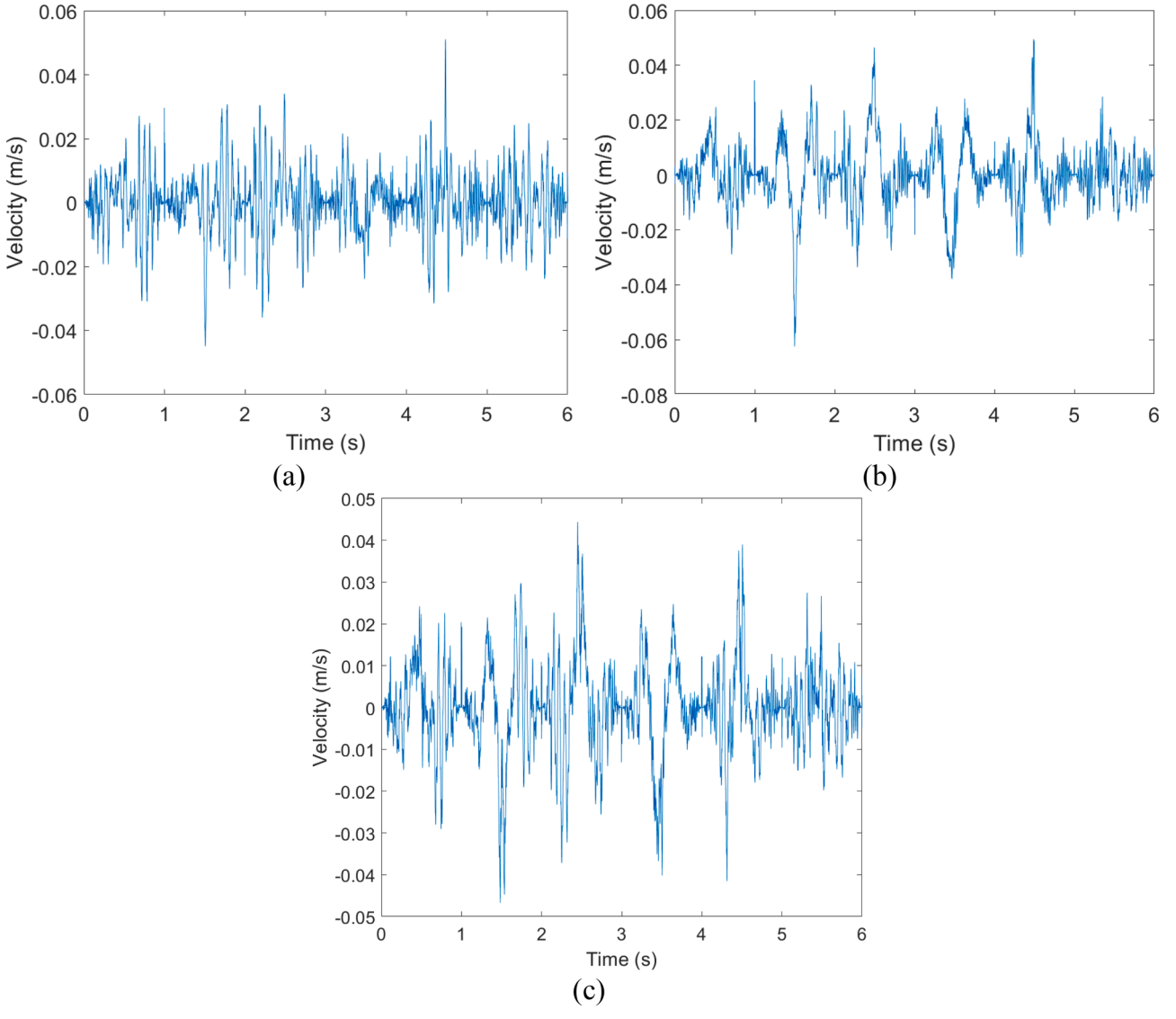

Fig. 3. Simulated CSLDV measurements when the distance between the random force excitation and the fixed end of the beam is (a) $x_q = 0.37$ m, (b) $x_q = 0.7$ m, and (c) $x_q = 1$ m.

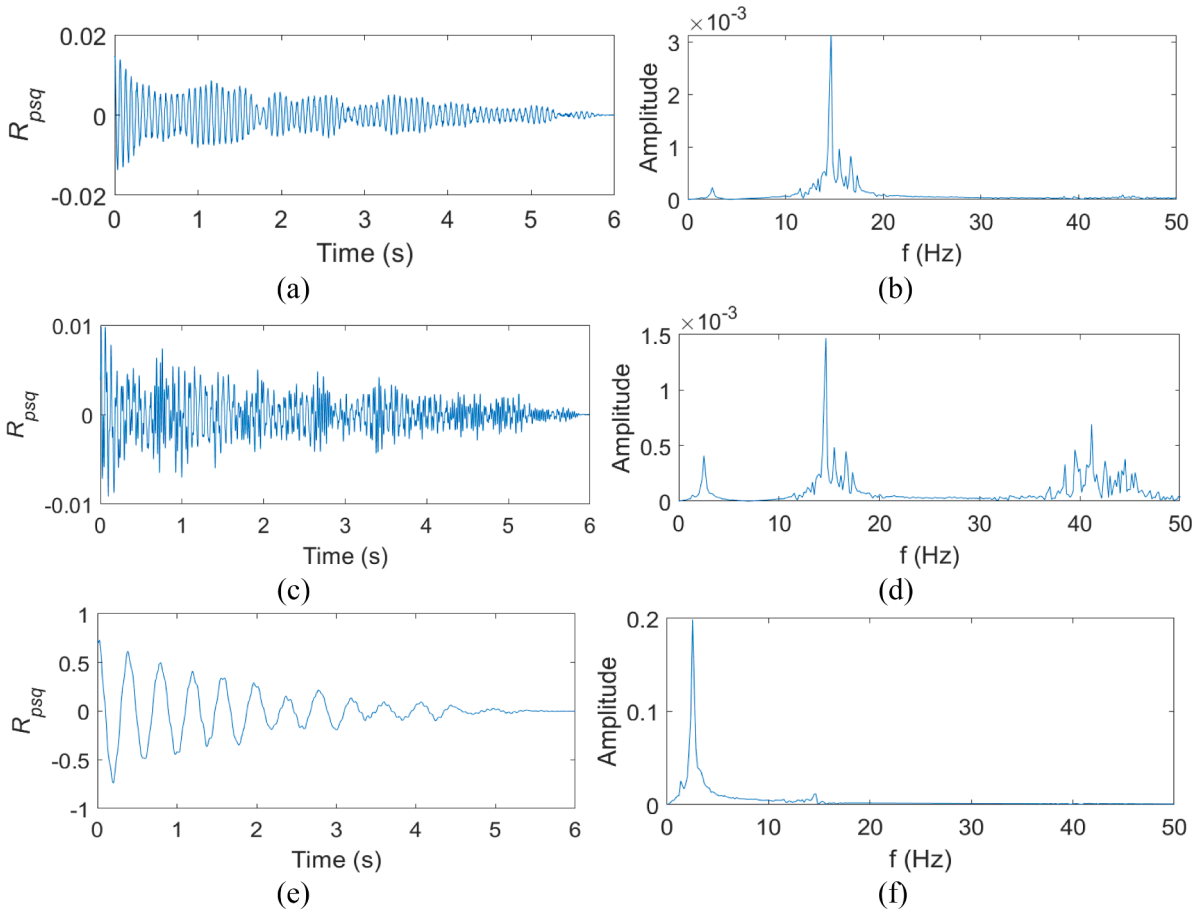

Fig. 4. (a) Correlation function between simulated CSLDV measurements with $x_q = 0.37$ m and the response of the node with η=0.5 and its frequency spectrum in (b), (c) the correlation function between simulated CSLDV measurements with $x_q = 0.7$ m and the response of the node with η = 0.7 and its frequency spectrum in (d), and (e) the correlation function between simulated CSLDV measurements with $x_q = 1$ m and the response of the node with η=0.9 and its frequency spectrum in (f).

denote 13 instants and integer numbers from 1 to 65 denote simulated responses (Fig. 2). Responses 1, 7, 13, 19, and 25 are chosen as measured responses when the laser spot of the CSLDV system sweep from node 1 to node 5 at instants t1, t2, t3, t4, and t5 (see the dashed line in Fig. 2). Similarly, responses 25, 29, 33, 37, and 41 are chosen as measured responses when the laser spot sweeps from node 5 to node 1 at instants t5, t6, t7, t8, and t9. The above preprocess scheme can be applied to any simulated responses with certain nodes and instants to simulate measured responses of a CSLDV system. The response of a node can be used as a reference signal to calculate a correlation function. Note that for estimating a mode shape of the beam, one needs to apply a random excitation on a node that is not at a nodal point of the mode shape, and choose the response of a node that is not at a nodal point of the mode shape as a reference signal.

Finite element simulation results

Simulated CSLDV measurements of the finite element model had a sampling frequency of 1000 Hz. Different excitation positions were used for estimating the first three bending modes of the beam, and simulated CSLDV measurements are shown in Fig. 3. Based on the preprocess scheme in Fig. 2 and the sampling frequency being $f_{sa} = 1,000$ Hz, the scan frequency, which is the number of completed scans in one second, is $f_{sc} = 1$ Hz. Note that the Nyquist frequency of a CSLDV measurement is half of the sampling frequency of the laser in the CSLDV system, but the number of measurement points n in a complete scan depends on both the sampling frequency and the scan frequency: $n = f_{sa}/f_{sc}$, which means that increasing f_{sa} and decreasing f_{sc} can both increase n. Once n is increased, the spatial resolution of an undamped mode shape that is estimated from the CSLDV measurement is increased, and one can obtain more accurate OMA results and damage detection results.

Responses at nodes of the finite element model were used as reference signals for calculating correlation functions. The method for calculation of correlation functions that is used in this work is an accurate and efficient calculation method of discrete correlation functions that was developed in Ref. [35]. Proper nodes are needed for estimating an undamped mode shape. Responses at nodes

Table 1
Estimated damped natural frequencies of the beam.

	First damped natural frequency (Hz)	Second damped natural frequency (Hz)	Third damped natural frequency (Hz)
FFT	2.50	14.67	42.50
FEM	2.46	14.89	42.56
Difference	1.63 %	1.48 %	0.14 %

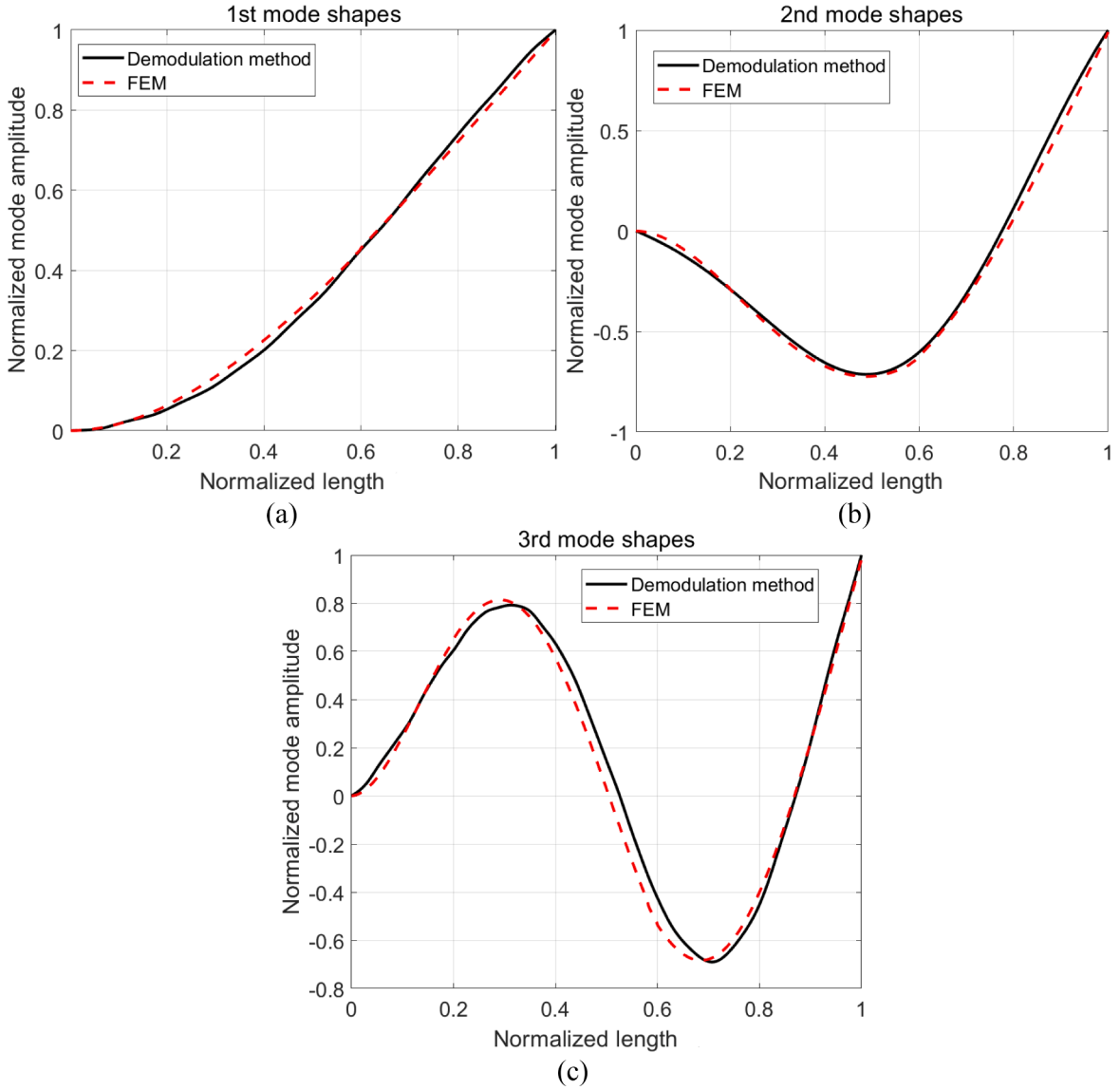

Fig. 5. Estimated (a) first, (b) second, and (c) third undamped mode shapes of the beam using the demodulation method and FEM.

where the undamped mode shape has a large amplitude while other undamped mode shapes have smaller amplitudes are suitable for estimating the undamped mode shape. Correlation functions between simulated CSLDV measurements in Fig. 3 and responses at nodes, and their frequency spectra are shown in Fig. 4. The correlation function in Fig. 4(a) can be used for estimating the second undamped mode shape since it has a large amplitude at the node with $x_q = 0.5$ m. Similarly, the correlation function in Fig. 4(c) can be used for estimating the third undamped mode shape, and the correlation function in Fig. 4(e) can be used for estimating the first undamped mode shape.

FFTs of obtained CSLDV measurements were used to determine damped natural frequencies of the beam (Table 1), and obtained correlation functions were processed by the demodulation method to estimate undamped mode shapes of the beam. To validate

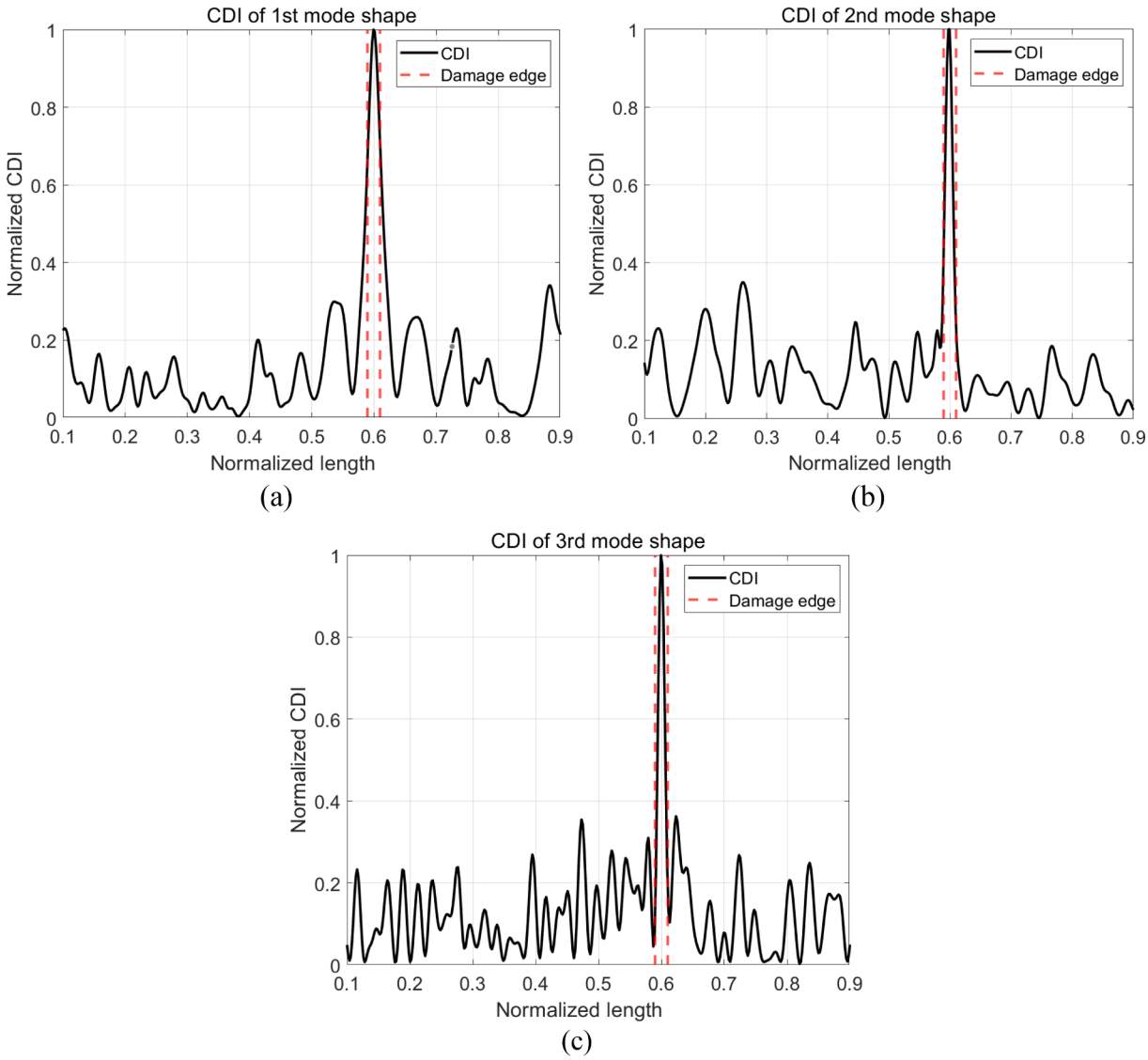

Fig. 6. Estimated averaged and normalized CDIs from (a) first, (b) second, and (c) third undamped mode shapes of the beam.

estimated damped natural frequencies and undamped mode shapes, modal analysis of the finite element model in ABAQUS was used to estimate damped natural frequencies and undamped mode shapes of the beam. Estimated first three undamped mode shapes of the beam using the demodulation method and FEM are compared in Fig. 5.

Modal assurance criterion (MAC) values between estimated first, second, and third undamped mode shapes of the beam using the demodulation method with a reference signal and FEM are 99.92 %, 99.57 %, and 98.79 %, respectively. The demodulation method with a reference signal can accurately estimate modal parameters of the beam based on differences in Table 1 and MAC values. The baseline-free damage detection method was applied to estimated undamped mode shapes using the demodulation method with a reference signal, and averaged and normalized CDIs are shown in Fig. 6. CDIs in ranges [0, 0.1] and [0.9, 1] were disregarded to eliminate effects of spurious boundary anomalies.[36] The highest peak in CDI plots in Fig. 6 are at the location of the damage in the beam; the location the damage in the beam was accurately estimated using the demodulation method with a reference signal and baseline-free damage detection method.

Experimental investigation

Experimental setup

A CSLDV system extended from a Polytec PSV-500–3D SLDV system was used to conduct experimental investigation on OMA and

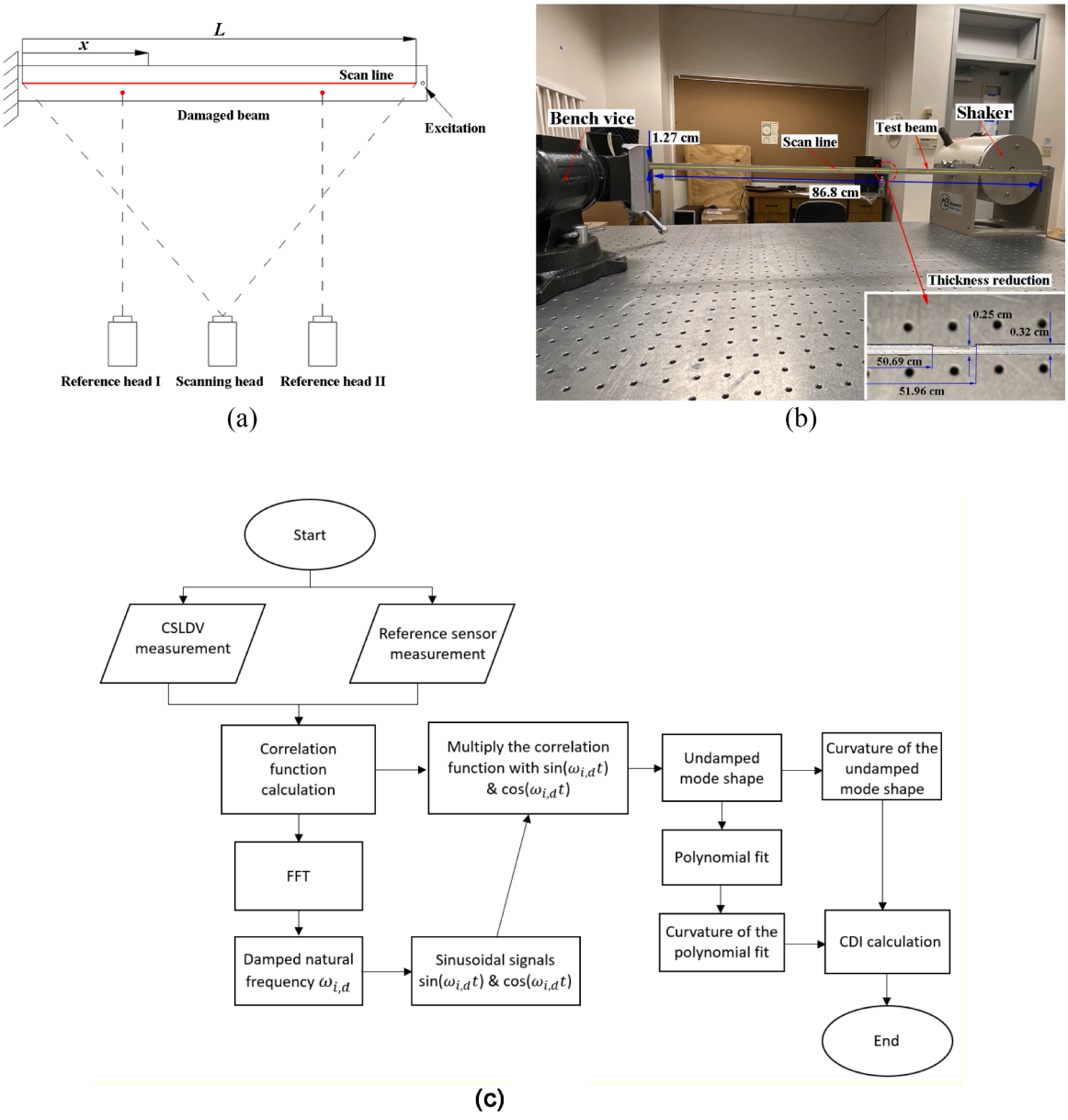

Fig. 7. (a) Schematic of experimental investigation on OMA and damage detection methods proposed in this work, (b) the experimental setup of the beam with a thickness reduction damage, and (c) the algorithmic diagram of the demodulation method with a reference signal for OMA and damage detection.

damage detection methods proposed in this work. An aluminum beam with a thickness reduction on its backside was used as the test structure in the experiment. The CSLDV system consisted of an external controller and three laser heads, which were referred to as the scanning head and reference heads I and II based on their roles during the test, as shown in Fig. 7(a). Mirrors of the scanning head were controlled by the external controller dSPACE MicroLabBox to continuously rotate, so that its laser spot can continuously scan along a pre-designed scan line on the surface of the damaged beam. Laser spots of reference heads were fixed on the surface of the damaged beam to capture vibrations of reference points.

The experimental setup of the CSLDV measurement of the damaged beam is shown in Fig. 7(b). One end of the beam was clamped by a bench vice and the other end was connected to a stinger of a MB Dynamics modal-50 shaker. A white-noise signal was input into the shaker to provide excitation. The thickness reduction damage on the backside of the beam was zoomed in and shown on the right bottom part of Fig. 7(b). The reduced thickness is about 21.8 % of the full thickness of the beam. One can see from Fig. 7 that $L = 86.8$ cm, and the damaged area started at $\eta = 0.584$ and ended at $\eta = 0.598$, meaning that its length is about 1.4 % of the full length of the scan line. The scanning frequency of CSLDV measurements was $f_{sc} = 1$ Hz, and its sampling frequency was $f_{sa} = 1{,}000$ Hz, which

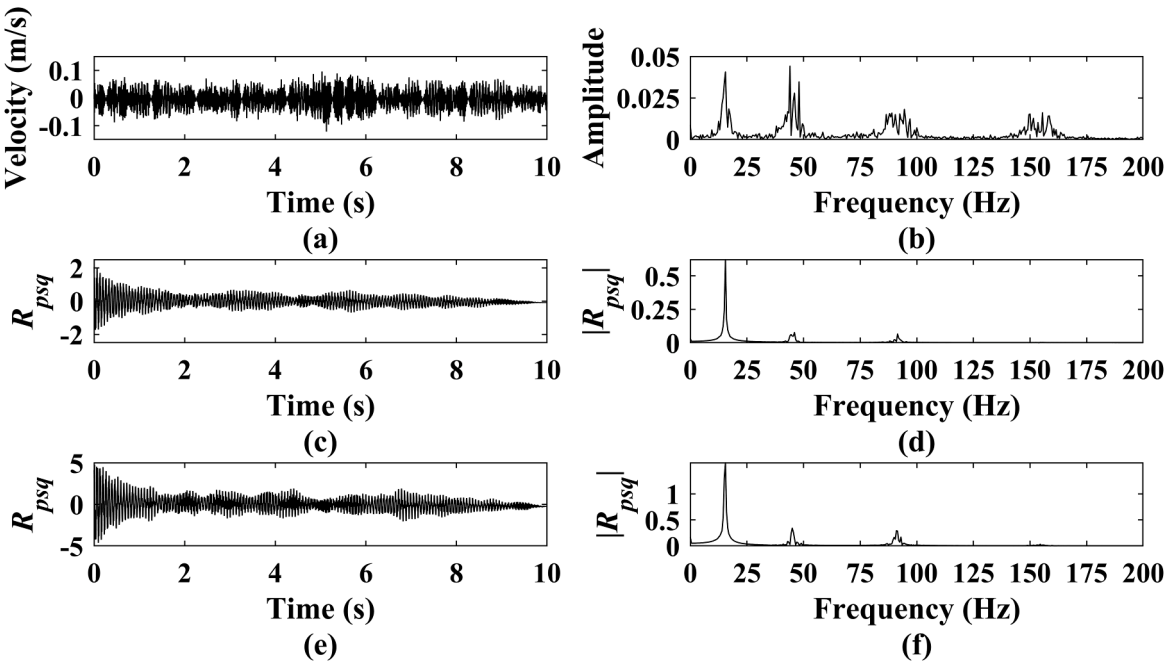

Fig. 8. (a) Vibration of the damaged beam under random excitation from CSLDV measurements and (b) its frequency spectrum, (c) the correlation function between the response in (a) and the reference response at η=0.3 and (d) its frequency spectrum, and (e) the correlation function between the response in (a) and the reference response at η=0.8 and (f) its frequency spectrum.

provided a total number of $N = f_{sa}/2f_{sc} = 500$ measurement points on the scan line. A modal test using the SLDV system was conducted in a step-wise way on the damaged beam with the same experimental setup as that shown in Fig. 7(b) to obtain its first three damped natural frequencies and mode shapes, which were compared with corresponding results from CSLDV measurements to validate the proposed OMA method. An algorithmic diagram of the demodulation method with a reference signal for OMA and damage detection is shown in Fig. 7(c).

Experimental results of modal parameter estimation and damage detection

Vibrations of points at $\eta = 0.3$ and $\eta = 0.8$ were selected as two references in the experiment to avoid nodal points of the first three modes of the damaged beam, and correlation functions R_{psq} between them and vibrations from the scanning head were obtained. In one set of measurements, vibrations with a duration of 10 s were captured by reference and scanning heads. The first step of modal parameter estimation of the damaged beam is to identify its damped natural frequencies. The vibration of the damaged beam under white-noise excitation from CSLDV measurements is shown in Fig. 8(a) and its frequency spectrum is shown in Fig. 8(b). One can see that it is difficult to directly identify damped natural frequencies of the beam from its frequency spectrum due to the low signal-to-noise ratio of the response of the beam under white-noise excitation. Correlation functions using references at $\eta = 0.3$ and $\eta = 0.8$ are shown in Fig. 8(c) and (e), respectively, and their frequency spectra are shown in Fig. 8(d) and (f), respectively. The first three damped natural frequencies of the damaged beam can be identified from frequency spectra of correlation functions in the two cases. As listed in Table 2, the maximum absolute error between the first three damped natural frequencies of the beam from SLDV measurements and those from CSLDV measurements with the reference at $\eta = 0.3$ is 1.3 %, and that for $\eta = 0.8$ is 0.9 %.

Based on Eq. (12) in Section 'Demodulation method for the correlation function', undamped mode shapes of the damaged beam can be estimated from correlation functions shown in Fig. 8 using its identified natural frequencies and the demodulation method with a reference signal. In this work, the first three undamped mode shapes of the beam were estimated from CSLDV measurements with

Table 2
Comparison between damped natural frequencies of the damaged beam from SLDV measurements and those from CSLDV measurements with references at $\eta = 0.3$ and $\eta = 0.8$.

Mode No.	SLDV measurement	CSLDV measurement with reference			
		η=0.3	Error	η=0.8	Error
1	15.6 Hz	15.5 Hz	−0.6 %	15.7 Hz	0.6 %
2	45.0 Hz	45.2 Hz	0.4 %	44.6 Hz	0.9 %
3	91.3 Hz	90.1 Hz	−1.3 %	91.7 Hz	0.4 %

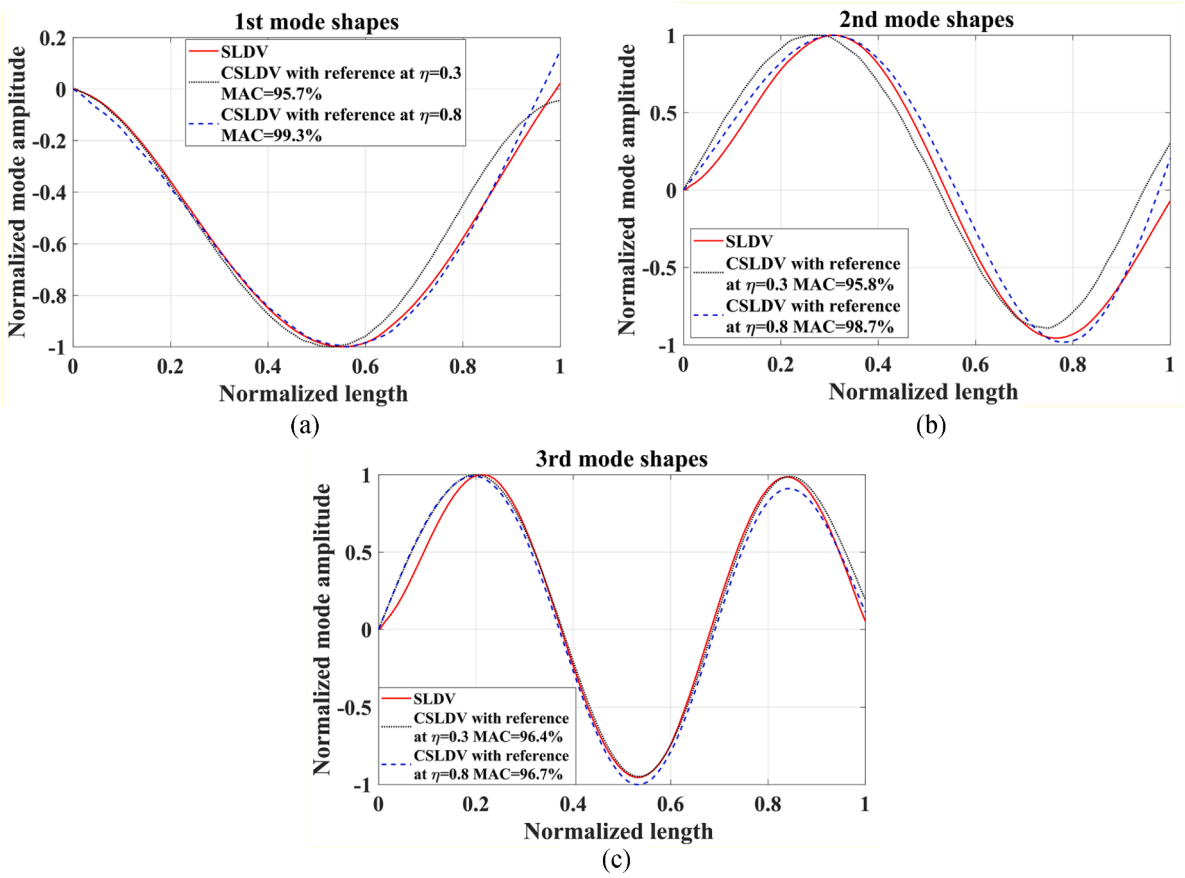

Fig. 9. Comparisons between estimated mode shapes of the damaged beam from SLDV measurements and those from CSLDV measurements with references at η=0.3 and η=0.8 for its (a) first mode, (b) second mode, and (c) third mode.

references at $\eta = 0.3$ and $\eta = 0.8$ and compared with those from SLDV measurements, as shown in Fig. 9, where red solid lines denote mode shapes from SLDV measurements, and black dotted lines and blue dashed lines denote mode shapes from CSLDV measurements with references at $\eta = 0.3$ and $\eta = 0.8$, respectively. One can see that MAC values between the first three mode shapes of the beam from SLDV and CSLDV measurements are larger than 95.7 % when $\eta = 0.3$, and larger than 96.7 % when $\eta = 0.8$.

In order to reduce the noise of damage detection results, the set of vibration data with a duration of 10 s captured in CSLDV measurements with a reference signal was split in ten sets with durations of 1 s. Ten CDIs were calculated using Eq. (17) for each mode, and normalization and averaging were conducted on them to obtain final CDI results using Eq. (18) where $m = 10$ in the experiment. As shown in Fig. 10, the location of damage can be identified from peaks of CDI results from CSLDV measurements with references at $\eta = 0.3$ and $\eta = 0.8$. Note that the noise of CDI results for $\eta = 0.8$ was slightly smaller than that for $\eta = 0.3$.

Based on experiment results, the demodulation method with a reference signal and the baseline-free damage detection method can be used for high-accuracy damage location identification of a beam structure under random excitation, while the traditional demodulation method cannot. However, the demodulation method with a reference signal requires both a CSLDV system and a sensor for measuring responses of the structure. Moreover, to estimate multiple modes of a structure, reference signals measured from multiple positions on the structure are needed to increase signal-to-noise ratios of measured reference signals. If only one position is used for a reference signal, the position may be close to a nodal point of a measured mode shape of the structure so that the signal-to-noise ratio of the measured reference signal is too low for estimating the mode shape. The frequency spectrum in Fig. 4(b) can only be used for identifying the second damped natural frequency of the finite element model since the amplitude of the second undamped mode shape is large at the reference node while amplitudes of the other two undamped mode shapes are small. The frequency spectrum of the correlation function between the response from the scanning head and the reference response at η=0.5 is shown in Fig. 11. One can see that the second natural frequency of the beam cannot be identified from the frequency spectrum, since η=0.5 is close to the nodal point of the second mode shape of the beam. The demodulation method with a reference signal is more complicated than the traditional demodulation method.

The lifting method can also be used for damage location identification of a beam structure under random excitation, but it has some more limitation than the demodulation method with a reference signal. The lifting method requires the laser spot of the CSLDV system to sweep along prescribed scan paths with a sufficiently high speed. The Nyquist frequency of the CSLDV system when using the lifting

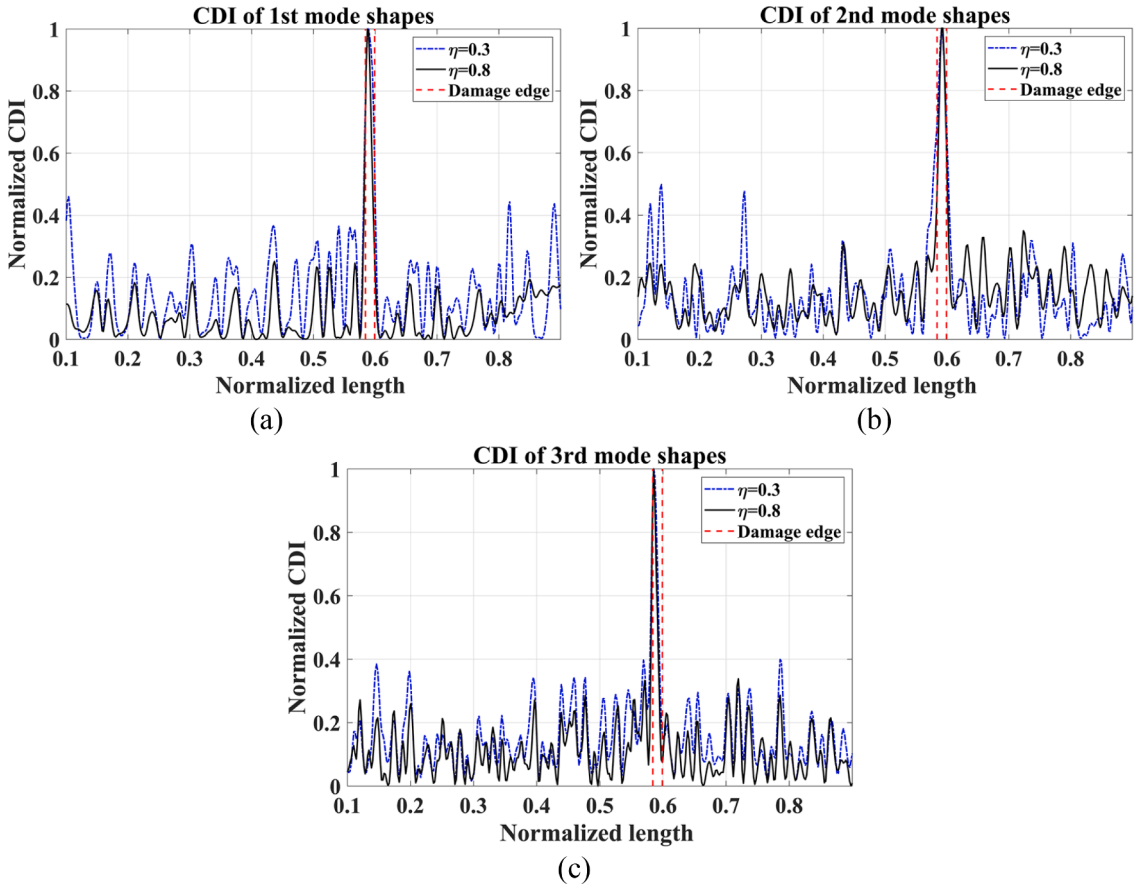

Fig. 10. Estimated averaged and normalized CDIs from CSLDV measurements with references at $\eta = 0.3$ and $\eta = 0.8$ for the (a) first mode, (b) second mode, and (c) third mode of the damaged beam.

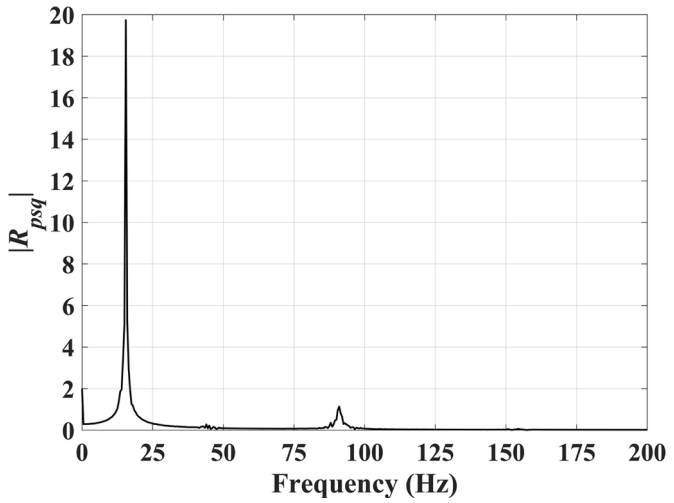

Fig. 11. Frequency spectrum of the correlation function between the response from the scanning head and the reference response at η=0.5.

method is equal to its scanning frequency, which means that it is difficult to use the CSLDV system to estimate modal parameters of a structure with high natural frequencies. It is also difficult to use the lifting method for a 2D scan since scanning along a 2D path takes much more time than scanning along a 1D path, which greatly reduces the scanning frequency of the CSLDV system. Moreover, measured responses of the lifting method are reconstructed to measured responses at multiple measurement points as if there were

sensors attached to these points. The spatial resolution of the lifting method depends on the number of measurement points. Measured responses at measurement points need to be separately processed, which can take much time for processing if the spatial resolution of the lifting method is high. The demodulation method with a reference signal can estimate modal parameters of a structure with high natural frequencies since the Nyquist frequency of the CSLDV system when using the demodulation method with a reference signal depends on the sampling frequency of the system. The demodulation method with a reference signal can be extended to a 2D scan, which will be studied in the future.

Conclusion

A novel demodulation method with a reference signal is developed for processing measured responses of a damaged structure under random excitation by a CSLDV system. Correlation functions between CSLDV measurements and measured responses at a reference point are calculated and multiplied by sinusoidal signals whose frequencies are damped natural frequencies of the structure. Multiplied correlation functions are filtered by low pass filters to obtain undamped mode shapes of the structure. A baseline-free damage detection method is used to calculate curvatures of estimated undamped mode shapes and compare obtained curvatures with curvatures of polynomial-fitted undamped mode shapes. CDIs are calculated, which can show the location of a damage in the structure. Both numerical and experimental investigations are conducted to validate the novel demodulation method with a reference signal and baseline-free damage detection method. Locations of damages in beams are accurately estimated in numerical and experimental investigations. Some limitations of the damage detection method are that damages at the boundary of the structure cannot be detected by the damage detection method since CDIs in ranges [0, 0.1] and [0.9, 1] were disregarded to eliminate effects of spurious boundary anomalies, and extents of damages are not explicitly provided in estimated CDIs. The novel demodulation method with a reference signal can be used for structural health monitoring of a beam structure under random excitation by processing measurements from a CSLDV system with a low scan frequency and a reference sensor, while the previous demodulation method and lifting method cannot.

CRediT authorship contribution statement

L.F. Lyu: Methodology, Software, Validation, Writing – original draft. **K. Yuan:** Methodology, Software, Validation, Writing – original draft. **W.D. Zhu:** Conceptualization, Methodology, Funding acquisition, Supervision, Validation, Writing – review & editing.

Declaration of Competing Interest

The authors declare that they have no known competing financial interests or personal relationships that could have appeared to influence the work reported in this paper.

Data availability

Data will be made available on request.

Acknowledgment

This research was supported by the National Science Foundation through grant no. CMMI-1763024.

References

[1] D.J. Ewins, Modal Testing: Theory and Practice, 15, Research studies press, Letchworth, 1984.
[2] Y.F. Xu, W.D. Zhu, Efficient and accurate calculation of discrete frequency response functions and impulse response functions, J Vib Acoust 138 (3) (2016), 031003, https://doi.org/10.1115/1.4031998.
[3] S.D. Valdes, C. Soutis, Delamination detection in composite laminates from variations of their modal characteristics, J Sound Vib 228 (1) (1999) 1–9, https://doi.org/10.1006/jsvi.1999.2403.
[4] W. Lestari, P. Qiao, S. Hanagud, Curvature mode shape-based damage assessment of carbon/epoxy composite beams, J Intell Mater Syst Struct 18 (3) (2007) 189–208, https://doi.org/10.1177/1045389x06064355.
[5] M. He, T. Yang, Y. Du, Nondestructive identification of composite beams damage based on the curvature mode difference, Compos Struct 176 (2017) 178–186, https://doi.org/10.1016/j.compstruct.2017.05.040.
[6] S. Rothberg, M. Allen, P. Castellini, An international review of laser Doppler vibrometry: making light work of vibration measurement, Opt Laser Eng 99 (1) (2017) 11–22, https://doi.org/10.1016/j.optlaseng.2016.10.023.
[7] B. Stoffregen, A. Felske, Scanning laser Doppler vibration analysis system, SAE Transact 94 (2) (1985) 934–940, 1985.
[8] P. Castellini, M. Martarelli, E. Tomasini, Laser Doppler vibrometry: development of advanced solutions answering to technology's needs, Mech Syst Signal Process 20 (6) (2006) 1265–1285, https://doi.org/10.1016/j.ymssp.2005.11.015.
[9] K. Yuan, W. Zhu, Modeling of welded joints in a pyramidal truss sandwich panel using beam and shell finite elements, J Vib Acoust 143 (4) (2021), 041002, https://doi.org/10.1115/1.4048792.
[10] C. Vuye, S. Vanlanduit, F. Presezniak, G. Steenackers, P. Guillaume, Optical measurement of the dynamic strain field of a fan blade using a 3D scanning vibrometer, Opt Lasers Eng 49 (7) (2011) 988–997, https://doi.org/10.1016/j.optlaseng.2011.01.021.
[11] P. Sriram, S. Hanagud, J. Craig, N.M. Komerath, Scanning laser Doppler technique for velocity profile sensing on a moving surface, Appl Opt 29 (16) (1990) 2409–2417, https://doi.org/10.1364/AO.29.002409.
[12] P. Sriram, S. Hanagud, J. Craig, Mode shape measurement using a scanning laser Doppler vibrometer, Int J Anal Exp Modal anal 7 (3) (1992) 169–178.

[13] M.S. Allen, M.W. Sracic, A new method for processing impact excited continuous-scan laser Doppler vibrometer measurements, Mech Syst Signal Process 24 (3) (2010) 721–735, https://doi.org/10.1016/j.ymssp.2009.11.004.
[14] D.M. Chen, Y.F. Xu, W.D. Zhu, Damage identification of beams using a continuously scanning laser Doppler vibrometer system, J Vib Acoust 138 (5) (2016) 05011, https://doi.org/10.1115/1.4033639.
[15] L.F. Lyu, W.D. Zhu, Operational modal analysis of a rotating structure under ambient excitation using a tracking continuously scanning laser Doppler vibrometer system, Mech Syst Signal Process 152 (2021), 107367, https://doi.org/10.1016/j.ymssp.2020.107367.
[16] L.F. Lyu, G.D. Higgins, W.D. Zhu, Operational modal analysis of a rotating structure using image-based tracking continuously scanning laser Doppler vibrometry via a novel edge detection method, J Sound Vib 525 (2022), 116797, https://doi.org/10.1016/j.jsv.2022.116797.
[17] D.M. Chen, W.D. Zhu, Investigation of three-dimensional vibration measurement by three scanning laser Doppler vibrometers in a continuously and synchronously scanning mode, J Sound Vib 498 (2021), 115950, https://doi.org/10.1016/j.jsv.2021.115950.
[18] K. Yuan, W.D. Zhu, Estimation of modal parameters of a beam under random excitation using a novel 3D continuously scanning laser Doppler vibrometer system and an extended demodulation method, Mech Syst Signal Process 155 (2021), 107606, https://doi.org/10.1016/j.ymssp.2021.107606.
[19] K. Yuan, W.D. Zhu, In-plane operating deflection shape measurement of an aluminum plate using a three-dimensional continuously scanning laser Doppler vibrometer system, Exp Mech 62 (2022) 667–676, https://doi.org/10.1007/s11340-021-00801-x.
[20] K. Yuan, W.D. Zhu, A novel general-purpose three-dimensional continuously scanning laser Doppler vibrometer system for full-field vibration measurement of a structure with a curved surface, J Sound Vib 540 (2022), 117274, https://doi.org/10.1016/j.jsv.2022.117274.
[21] K. Yuan, W.D. Zhu, Identification of modal parameters of a model turbine blade with a curved surface under random excitation with a three-dimensional continuously scanning laser Doppler vibrometer system, Measurement (2023), 112759, https://doi.org/10.1016/j.measurement.2023.112759.
[22] A. Stanbridge, D. Ewins, Modal testing using a scanning laser Doppler vibrometer, Mech Syst Signal Process 13 (2) (1999) 255–270, https://doi.org/10.1006/mssp.1998.1209.
[23] D. Di Maio, D. Ewins, Continuous scan, a method for performing modal testing using meaningful measurement parameters; Part I, Mech Syst Signal Process 25 (8) (2011) 3027–3042, https://doi.org/10.1016/j.ymssp.2011.05.018.
[24] Y.F. Xu, D.M. Chen, W.D. Zhu, Damage identification of beam structures using free response shapes obtained by use of a continuously scanning laser Doppler vibrometer system, Mech Syst Signal Process 92 (2017) 226–247, https://doi.org/10.1016/j.ymssp.2016.12.042.
[25] Y.F. Xu, D.M. Chen, W.D. Zhu, Modal parameter estimation using free response measured by a continuously scanning laser Doppler vibrometer system with application to structural damage identification, J Sound Vib 485 (2020), 115536, https://doi.org/10.1016/j.jsv.2020.115536.
[26] S. Yang, M.S. Allen, Lifting approach to simplify output-only continuous-scan laser vibrometry, Mech Syst Signal Process 45 (2) (2014) 267–282, https://doi.org/10.1016/j.ymssp.2013.11.010.
[27] Y.F. Xu, D.M. Chen, W.D. Zhu, Operational modal analysis using lifted continuously scanning laser Doppler vibrometer measurements and its application to baseline-free structural damage identification, J Vib Control 25 (7) (2019) 1341–1364, https://doi.org/10.1177/1077546318821154.
[28] D.M. Chen, Y.F. Xu, W.D. Zhu, Experimental investigation of notch-type damage identification with a curvature-based method by using a continuously scanning laser Doppler vibrometer system, J Nondestruct Eval 36 (2) (2017) 38, https://doi.org/10.1007/s10921-017-0418-4.
[29] D.M. Chen, Y.F. Xu, W.D. Zhu, Identification of damage in plates using full-field measurement with a continuously scanning laser Doppler vibrometer system, J Sound Vib 422 (2018) 542–567, https://doi.org/10.1016/j.jsv.2018.01.005.
[30] D. Chen, Y.F. Xu, W.D. Zhu, Non-model-based identification of delamination in laminated composite plates using a continuously scanning laser Doppler vibrometer system, J Vib Acoust 140 (4) (2018), 041001, https://doi.org/10.1115/1.4038734.
[31] D.M. Chen, Y.F. Xu, W.D. Zhu, A comprehensive study on detection of hidden delamination damage in a composite plate using curvatures of operating deflection shapes, J Nondestruct Eval 38 (2019) 54, https://doi.org/10.1007/s10921-019-0591-8.
[32] Z. Huang, C. Zang, Damage Detection Using Modal Rotational Mode Shapes Obtained with a Uniform Rate CSLDV Measurement, Appl Sci 9 (23) (2019) 4982, https://doi.org/10.3390/app9234982.
[33] L.F. Lyu, W.D. Zhu, Operational modal analysis of a rotating structure subject to random excitation using a tracking continuously scanning laser Doppler vibrometer via an improved demodulation method, ASME J Vib Acoust 144 (1) (2021), 011006, https://doi.org/10.1115/1.4051178.
[34] L.F. Lyu, W.D. Zhu, Full-field mode shape estimation of a rotating structure subject to random excitation using a tracking continuously scanning laser Doppler vibrometer via a two-dimensional scan scheme, Mech Syst Signal Process 169 (2022), 108532, https://doi.org/10.1016/j.ymssp.2021.108532.
[35] Y.F. Xu, J.M. Liu, W.D. Zhu, Accurate and efficient calculation of discrete correlation functions and power spectra, J Sound Vib 347 (2015) 246–265, https://doi.org/10.1016/j.jsv.2015.02.026.
[36] D. Di Maio, P. Castellini, M. Martarelli, S. Rothberg, M.S. Allen, W.D. Zhu, D.J. Ewins, Continuous Scanning Laser Vibrometry: a raison d'être and applications to vibration measurements, Mech Syst Signal Process 156 (2021), 107573, https://doi.org/10.1016/j.ymssp.2020.107573.